Extracting Quantum Work Statistics and Fluctuation Theorems by Single-Qubit Interferometry

R. Dorner,[1,2,*] S. R. Clark,[2,3] L. Heaney,[3] R. Fazio,[3,4] J. Goold,[2,5] and V. Vedral[2,3]

[1]*Blackett Laboratory, Imperial College London, Prince Consort Road, London SW7 2AZ, United Kingdom*
[2]*Clarendon Laboratory, University of Oxford, Parks Road, Oxford OX1 3PU, United Kingdom*
[3]*Centre for Quantum Technologies, National University of Singapore, 3 Science Drive 2, Singapore 117543*
[4]*NEST, Scuola Normale Superiore and Istituto Nanoscienze-CNR, I-56126 Pisa, Italy*
[5]*Department of Physics, University College Cork, Cork, Ireland*

(Received 11 February 2013; revised manuscript received 29 April 2013; published 7 June 2013)

We propose an experimental scheme to verify the quantum nonequilibrium fluctuation relations using current technology. Specifically, we show that the characteristic function of the work distribution for a nonequilibrium quench of a general quantum system can be extracted by Ramsey interferometry of a single probe qubit. Our scheme paves the way for the full characterization of nonequilibrium processes in a variety of quantum systems, ranging from single particles to many-body atomic systems and spin chains. We demonstrate our idea using a time-dependent quench of the motional state of a trapped ion, where the internal pseudospin provides a convenient probe qubit.

DOI: 10.1103/PhysRevLett.110.230601 PACS numbers: 05.70.Ln

Introduction.—In the past two decades, the discovery of the nonequilibrium fluctuation relations has made a significant contribution to understanding the full nonlinear response of a microscopic system subject to a time-dependent force [1–4]. Initially, these relations were derived for classical systems and experimentally confirmed in single-molecule stretching experiments [5]. More recently, their extension to the quantum regime has lead to theoretical progress in understanding the microscopic underpinnings of the laws of thermodynamics [6,7]. Notably, however, an experimental verification of the quantum fluctuation relations is still forthcoming.

In this Letter, we propose an experimental scheme to extract the full statistics of work done in a nonequilibrium transformation of an arbitrary closed quantum system. The crux of our proposal is that the characteristic function of the work distribution can be extracted via Ramsey interferometry of a probe qubit. Extracting the statistics of work in this way circumvents the requirement to perform projective energy measurements on the system of interest, as in previous proposals [8], making our scheme generally applicable to a range of systems, including Bose [9,10] and Fermi gases [11,12], spin chains [13], and quenched ion strings [14]. We demonstrate the feasibility of our proposal using realistic parameters for the example of a trapped ion interacting with an external laser field (see Ref. [15] for details of a similar scheme using hybrid optomechanical-electromechanical devices).

Nonequilibrium quantum thermodynamics.—We begin by considering a closed quantum system described by a Hamiltonian $\hat{H}(\lambda)$ containing an externally controlled parameter $\lambda(t)$. At time $t = 0$ the control parameter has the initial value $\lambda(0) = \lambda_\mathrm{i}$ and the system is prepared in the Gibbs state $\hat{\varrho}_\beta(\lambda_\mathrm{i}) = \exp[-\beta\hat{H}(\lambda_\mathrm{i})]/\mathcal{Z}_\beta(\lambda_\mathrm{i})$, where $\mathcal{Z}_\beta(\lambda) := \mathrm{tr}\{\exp[-\beta\hat{H}(\lambda)]\}$ is the partition function at inverse temperature β. The system is driven away from equilibrium by varying $\lambda(t)$ in a pre-defined, but otherwise arbitrary way, over the quench time interval t_Q to its final value $\lambda(t_\mathrm{Q}) = \lambda_\mathrm{f}$. The initial and final Hamiltonians have the spectral decompositions $\hat{H}(\lambda_\mathrm{i}) = \sum_n \epsilon_n |n\rangle\langle n|$ and $\hat{H}(\lambda_\mathrm{f}) = \sum_m \bar{\epsilon}_m |\bar{m}\rangle\langle\bar{m}|$, respectively, and the protocol $\hat{H}(\lambda_\mathrm{i}) \to \hat{H}(\lambda_\mathrm{f})$ that connects them generates the unitary evolution $\hat{U}(t_\mathrm{Q})$.

The work done on the system W is defined by two projective energy measurements: The first, at $t = 0$, projects onto the eigenbasis of $\hat{H}(\lambda_\mathrm{i})$ and gives the outcome ϵ_n with probability $p_n = \exp[-\beta\epsilon_n]/\mathcal{Z}_\beta(\lambda_\mathrm{i})$. The second measurement, at $t = t_\mathrm{Q}$, projects onto the eigenbasis of $\hat{H}(\lambda_\mathrm{f})$ and gives the outcome $\bar{\epsilon}_m$ with probability $p_{m|n} = |\langle\bar{m}|\hat{U}(t_\mathrm{Q})|n\rangle|^2$. The quantum work distribution, which encodes the random fluctuations in the nonequilibrium work, is given by

$$P_\mathrm{F}(W) := \sum_{n,m} p_n p_{m|n} \delta(W - (\bar{\epsilon}_m - \epsilon_n)). \tag{1}$$

Here "F" denotes that this is the work distribution for the forward process $\hat{H}(\lambda_\mathrm{i}) \to \hat{H}(\lambda_\mathrm{f})$. The corresponding backward work distribution $P_\mathrm{B}(W)$ is obtained by preparing the system in the Gibbs state $\hat{\varrho}_\beta(\lambda_\mathrm{f})$ of the final Hamiltonian and subjecting it to the time-reversed protocol $\hat{H}(\lambda_\mathrm{f}) \to \hat{H}(\lambda_\mathrm{i})$, which generates the evolution $\hat{\Theta}\hat{U}^\dagger(t_\mathrm{Q})\hat{\Theta}^\dagger$, where $\hat{\Theta}$ is the antiunitary time-reversal operator [16].

Important equilibrium information can be extracted by studying the fluctuations in nonequilibrium work. This is revealed by the nonequilibrium fluctuation relations, in particular, the Tasaki-Crooks relation [4,7]

$$\frac{P_\mathrm{F}(W)}{P_\mathrm{B}(-W)} = e^{\beta(W-\Delta F)}, \tag{2}$$

which shows that, for any closed quantum system undergoing an arbitrary nonequilibrium transformation, the fluctuations in work are related to the equilibrium free energy difference $\Delta F = (1/\beta)\ln[\mathcal{Z}_\beta(\lambda_i)/\mathcal{Z}_\beta(\lambda_f)]$.

In this Letter, the primary quantities of interest are the forward and backward characteristic functions, defined as the Fourier transform of the corresponding work distributions [17]. The forward characteristic function is, thus (taking $\hbar = 1$),

$$\chi_F(u) := \int dW e^{iuW} P_F(W), \\ = \mathrm{tr}[\hat{U}^\dagger(t_Q) e^{iu\hat{H}(\lambda_f)} \hat{U}(t_Q) e^{-iu\hat{H}(\lambda_i)} \hat{\varrho}_\beta(\lambda_i)], \quad (3)$$

while the backward characteristic function is $\chi_B(u) := \int dW e^{iuW} P_B(W)$.

Previous experimental proposals to extract the full statistics of work, and verify the quantum fluctuation theorems, have sought to directly measure the work distribution via a series of projective energy measurements [8]. However, even for systems of modest complexity this can be practically challenging. In the following, we show how this difficulty can be avoided by instead opting to measure the characteristic function using well-established experimental techniques.

Experimental extraction of the characteristic function.—The purpose of our proposal is to measure the work done in a nonequilibrium transformation of a generic quantum system by temporarily coupling it to an easily addressable probe qubit. We assume that the total Hamiltonian describing the qubit and system of interest has the form $\hat{H}_T(t) = (\Delta/2)\hat{\sigma}_z + \hat{H}_S + \hat{H}_I(t)$, where Δ is the splitting between the ground $|\downarrow\rangle$ and excited $|\uparrow\rangle$ states of the qubit, which are eigenstates of the spin-1/2 Pauli z operator $\hat{\sigma}_z$ (similarly $\hat{\sigma}_x$ and $\hat{\sigma}_y$ denote the Pauli x and y operators) and $\hat{H}_S$ is the time-independent Hamiltonian of the system of interest. The qubit-system interaction term $\hat{H}_I(t)$ contains all of the time dependence and is assumed to have the form

$$\hat{H}_I(t) = (g_\downarrow(t)|\downarrow\rangle\langle\downarrow| + g_\uparrow(t)|\uparrow\rangle\langle\uparrow|) \otimes \hat{V}, \quad (4)$$

where $g_\uparrow(t)$ and $g_\downarrow(t)$ are externally controlled parameters and $\hat{V}$ is a perturbation acting on the system of interest.

We note that the form of the interaction given in Eq. (4) allows the system of interest to be quenched as $\hat{H}(\lambda_i) = \hat{H}_S + \lambda_i\hat{V} \to \hat{H}(\lambda_f) = \hat{H}_S + \lambda_f\hat{V}$ by varying both of the spin-dependent parameters $g_\downarrow(t)$ and $g_\uparrow(t)$ according to $\lambda(t)$. However, to extract the characteristic function for this quench, the time dependent parameters must be independently varied according to a distinct Ramsey sequence over the time interval $t_R \geq t_Q$. Explicitly, the experimental procedure to extract the characteristic function is as follows: (i) For times $t \leq 0$ the qubit is decoupled from the system by holding the spin-dependent couplings fixed at $g_\downarrow(0) = g_\uparrow(0) = \lambda_i$. Furthermore, the qubit and system are thermalized in the product state $\hat{\rho} = |\downarrow\rangle\langle\downarrow| \otimes \varrho_\beta(\lambda_i)$ by ensuring that $\beta\Delta \gg 1$. (ii) At $t = 0$, a Hadamard operation $\hat{\sigma}_H = (\hat{\sigma}_x + \hat{\sigma}_z)/\sqrt{2}$ is applied to the qubit. (iii) The spin-dependent couplings are independently varied over the Ramsey time internal t_R as

$$g_\uparrow(t) = \begin{cases} \lambda(t), & 0 \leq t < t_Q \\ \lambda_f, & t_Q \leq t \leq t_R \end{cases} \\ g_\downarrow(t) = \begin{cases} \lambda_i, & 0 \leq t < t_R - t_Q \\ \lambda(t - t_R + t_Q), & t_R - t_Q \leq t \leq t_R. \end{cases} \quad (5)$$

This protocol generates the unitary evolution $\hat{T}(t_R)$ that acts in the joint Hilbert space of the qubit and system to generate a conditional dynamical quench of the system contingent upon the state of the probe qubit. Crucially, the quench is either followed or preceded by a period of constant evolution. (iv) At the end of the protocol $t = t_R$, we have $g_\downarrow(t_R) = g_\uparrow(t_R) = \lambda_f$, ensuring that the qubit and system are decoupled, and a second Hadamard operation is performed on the qubit.

The output state of the qubit at the end of the Ramsey sequence is

$$\hat{\rho}_q = \mathrm{tr}_S[\hat{\sigma}_H\hat{T}(t_R)\hat{\sigma}_H\hat{\rho}\hat{\sigma}_H\hat{T}^\dagger(t_R)\hat{\sigma}_H] \\ = \frac{1 + \Re[L(t_R)]}{2}|\downarrow\rangle\langle\downarrow| + \frac{i\Im[L(t_R)]}{2}|\downarrow\rangle\langle\uparrow| \\ - \frac{i\Im[L(t_R)]}{2}|\uparrow\rangle\langle\downarrow| + \frac{1 - \Re[L(t_R)]}{2}|\uparrow\rangle\langle\uparrow|, \quad (6)$$

where we have introduced the decoherence factor

$$L(t_R) = \mathrm{tr}_S[\hat{T}_\uparrow^\dagger(t_R)\hat{T}_\downarrow(t_R)\hat{\varrho}_\beta(\lambda_i)]. \quad (7)$$

Here, the unitary operators $\hat{T}_\downarrow(t_R) = \langle\downarrow|\hat{T}(t_R)|\downarrow\rangle$ and $\hat{T}_\uparrow(t_R) = \langle\uparrow|\hat{T}(t_R)|\uparrow\rangle$ act in the Hilbert space of the system and describe its evolution under the two different time-dependent quenches generated by $g_\downarrow(t)$ and $g_\uparrow(t)$, respectively. Consequently, the Ramsey sequence [depicted in Fig. 1(a)] creates an entangled state between the basis states of the probe qubit and the two quenched states of the system, $\hat{T}_\downarrow[\hat{\varrho}_\beta(\lambda_i)]\hat{T}_\downarrow^\dagger$ and $\hat{T}_\uparrow[\hat{\varrho}_\beta(\lambda_i)]\hat{T}_\uparrow^\dagger$. The real $\Re[L(t_R)]$ and imaginary $\Im[L(t_R)]$ parts of the decoherence factor define the populations and coherences of the probe qubit density matrix in Eq. (6) and are reconstructed by measuring $\hat{\sigma}_z$ and $\hat{\sigma}_y$ over many identical experimental runs.

The judicious choice of the couplings in Eq. (5), illustrated in Figs. 1(b) and 1(c), establishes a direct relationship between $L(t_R)$ and the characteristic function $\chi_F(u)$ corresponding to the quench protocol $\hat{H}(\lambda_i) \to \hat{H}(\lambda_f)$. Specifically, the conditional unitary evolutions of the system are given by

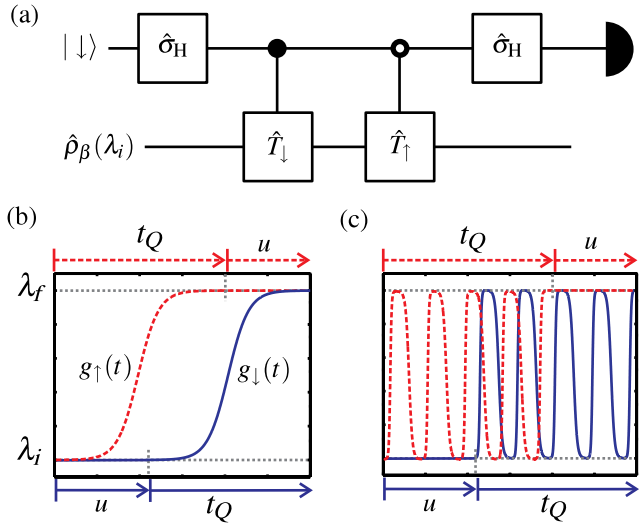

FIG. 1 (color online). (a) The Ramsey protocol represented as a quantum circuit. The probe qubit in the upper branch is prepared in the $|\downarrow\rangle$ state and the system of interest is prepared in the state $\varrho_\beta(\lambda_i)$ defined in the text. A black (white) circle indicates that the operation is controlled on the probe qubit being in the $|\downarrow\rangle$ ($|\uparrow\rangle$) state. Similar schemes are used in protocols for quantum parameter estimation [28]. In (b) and (c) examples are shown of the time variation of the spin-dependent couplings $g_\downarrow(t)$ and $g_\uparrow(t)$ over the Ramsey scheme time $t_R = t_Q + u$ required to obtain the characteristic function $\chi_F(u)$. In (b) a forward quench described by $\lambda(t) = \lambda_i + (\lambda_f - \lambda_i)[1 + \tanh(t/T)]/2$, where T is the switching time and the total quench time is $t_Q = 8T$, is shown. In (c) the forward quench is composed of repeated fast and slow tanh switches between λ_i and λ_f, as in (b), before ending at λ_f.

$$\hat{T}_\uparrow(t_R) = e^{-i(\Delta/2)t_R} e^{-i(t_R - t_Q)\hat{H}(\lambda_f)} \hat{U}(t_Q),$$
$$\hat{T}_\downarrow(t_R) = e^{i(\Delta/2)t_R} \hat{U}(t_Q) e^{-i(t_R - t_Q)\hat{H}(\lambda_i)}, \quad (8)$$

which, after identifying the time interval $u = t_R - t_Q$, show that the decoherence factor in Eq. (7) coincides with the forward characteristic function in Eq. (3) up to a known phase. Thus, the characteristic function is extracted by embedding the quench evolution $\hat{U}(t_Q)$ into the qubit-system evolution and repeating the protocol for different run times $t_R \geq t_Q$ [18]. The corresponding backwards characteristic function is obtained by a straightforward modification of the above scheme. In both cases, the work distributions $P_F(W)$ and $P_B(W)$ are obtained from the inverse Fourier transform of their respective characteristic functions [cf. Eq. (3)].

Implementation using a trapped ion.—We consider a single ion of mass M contained in a linear Paul trap [19]. By using the $S_{1/2}$ ground state Zeeman sublevels of the ion $|m = 1/2\rangle = |\uparrow\rangle$ and $|m = -1/2\rangle = |\downarrow\rangle$, this system provides an ideal realization of a spin-1/2 particle confined in a harmonic potential. We therefore have $\hat{H}_S = \omega_0(\hat{a}^\dagger\hat{a} + 1/2)$, where ω_0 is the natural frequency of the oscillator and $\hat{a}^\dagger$ ($\hat{a}$) is the oscillator raising (lowering) operator. Accurate detection of the ion's internal states can be accomplished by observing the scattered fluorescence from near-resonant driving of a cycling transition. Transformations between internal states can be implemented by a Raman transition (e.g., performing the Hadamard operation σ_H via a $\pi/2$ pulse) and the tunable azimuthal phase of the transition permits both $\langle\hat{\sigma}_z\rangle$ and $\langle\hat{\sigma}_y\rangle$ to be determined from the fixed final measurement [19]. Precise preparation of the initial thermal state $\hat{\varrho}_\beta$, with mean phonon number $\bar{n} = [\exp(\beta\omega_0) - 1]^{-1}$, can be achieved by allowing heating after resolved-sideband laser cooling to the motional ground state or Doppler cooling on the $S_{1/2}$ to $P_{1/2}$ transition [8,19].

The motional state of the ion is quenched by illuminating it with a far-detuned elliptically polarized standing wave laser field (see Ref. [20] for a similar procedure). Since the σ^+ and σ^- polarized contributions couple exclusively to the $|\downarrow\rangle$ and $|\uparrow\rangle$ states, respectively, they induce a spin-dependent optical dipole potential for the ion [21]. After making the rotating-wave approximation and adiabatically eliminating the far-detuned excited states, we obtain the interaction Hamiltonian [22]

$$\hat{H}_I = (\Omega_\downarrow(t)|\downarrow\rangle\langle\downarrow| + \Omega_\uparrow(t)|\uparrow\rangle\langle\uparrow|) \otimes \sin^2(k\hat{x} + \phi), \quad (9)$$

where k is the magnitude of the wave vector oriented along the trap axis for both polarizations, and ϕ is the phase of the standing waves relative to the trap centre at $x = 0$. The coupling parameters $\Omega_\uparrow(t)$ and $\Omega_\downarrow(t)$ are the time-dependent Rabi frequencies, which are individually controlled by varying the laser intensity for each polarization.

In the Lamb-Dicke regime, quantified by $\eta = kx_0 \ll 1$ where $x_0 = (2M\omega_0)^{-1/2}$, the extent of the ion's motion is small compared to the spatial variation of the optical dipole potential. Consequently, expanding $\hat{H}_I(t)$ to $O(\eta^3)$ around $x = 0$ gives an energy shift $\epsilon_\sigma(t) = \Omega_\sigma(t)\sin^2(\phi)$, a linear potential of strength $g_\sigma(t) = \eta\Omega_\sigma(t)\sin(2\phi)$ and a frequency change $\tilde{\omega}_\sigma = \omega_0 + 4\eta^2\Omega_\sigma(t)\cos(2\phi)$, where $\sigma = \{\uparrow, \downarrow\}$. By choosing the appropriate relative phase, the optical dipole potential can cause the oscillator to be tightened ($\phi = 0$), slackened ($\phi = \pi/2$) or displaced ($\phi = \pi/4$), while other phases lead to combinations of these effects. For concreteness, we focus on a pure displacement quench where the perturbation reduces to $\hat{V} = x_0(\hat{a}^\dagger + \hat{a})$ in addition to the energy shift $\epsilon_\sigma(t)$. Since $g_\sigma(t) \propto \Omega_\sigma(t)$, the protocol can be implemented by varying the laser intensities of the two orthogonally polarized standing waves.

The experimental verification of the Crooks relation in Eq. (2) was examined by numerically computing $\chi_F(u)$ and $\chi_B(u)$ for two different quenches in a possible $^{40}Ca^+$ ion experiment [21,23]. The following two experimental limitations were modeled; First, a realistic sampling rate for the measurement of $\chi_F(u)$ was used to account for discrete

data. Second, an enveloping factor $\exp(-u/\tau)$, with a decay time τ, was added to the measurement signal to account for decoherence of the entangled state that appears within the scheme [24]. Figure 2(a) shows the quantum work distributions $P_F(W)$ and $P_B(-W)$ for a forward quench described by a single tanh ramping [as shown in Fig. 1(b)] with the switching timescale T chosen to be a fraction of the natural trap frequency $2\pi/\omega_0$. Both $P_F(W)$ and $P_B(W)$ are composed of δ-peaks, separated by ω_0 and broadened into a continuous spectrum by the decoherence envelope. As the quench is nonquasistatic, the first-order peaks are visible, though much weaker than the carrier peak. Figure 2(b) shows the forward and backward work distributions for a quench composed of repeated fast and slow tanh switches [see Fig. 1(c)] with the fast switching on the order of a hundredth of $2\pi/\omega_0$. The stronger first-order peaks and now-visible second-order peaks evidence that this quench is highly nonquasistatic. In Fig. 2(c) we model an additional experimental limitation by computing the spectra for the same quench as Fig. 2(b) with 0.5% Gaussian noise added to $\chi_F(u)$ and $\chi_B(u)$. Despite this white noise, the first-order peaks remain visible.

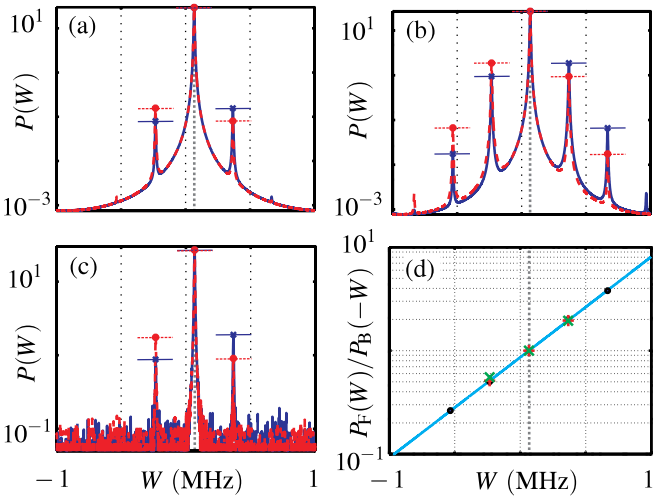

FIG. 2 (color online). A $^{40}Ca^+$ ion is assumed to be confined with an axial trapping frequency $\omega_0 = 300$ kHz and prepared in a thermal state with $\bar{n} = 1$. The standing wave optical dipole potential for both polarizations are taken as being generated by a 397 nm laser ≈ 30 GHz detuned from the $S_{1/2} - P_{1/2}$ transition, giving $\eta = 0.33$ and a maximum Rabi frequency of $\Omega = 150$ kHz [21,23]. A sampling rate of 2 MHz and a decoherence time scale of $\tau = 15 \times (2\pi/\omega_0) = 50$ μs has been used with measurements being performed up to a time ≈ 500 μs, where the signal was completely damped. (a) The quantum work distributions $P_F(W)$ (solid) and $P_B(-W)$ (dashed) are plotted on a logarithmic scale for a single tanh switching of $\lambda(t)$, as shown in Fig. 1(b), with $T = 0.3 \times (2\pi/\omega_0) = 1$ μs. The horizontal lines denote the peak amplitudes identified from both $P_F(W)$ and $P_B(-W)$. The vertical dashed lies at 67 kHz corresponding to the exact ΔF. (b) The plot as (a) for a repeated tanh switching quench, as shown in Fig. 1(c), with $T_{fast} = 0.2 \times (2\pi/\omega_0) = 0.03$ μs and $T_{slow} = 3 \times (2\pi/\omega_0) = 20$ μs. (c) The plot and quench as (b) with 0.5% Gaussian noise added to the signals for $\chi_F(u)$ and $\chi_B(u)$. (d) The ratio $P_F(W)/P_B(-W)$ was evaluated from the peaks identified in (a) (+), (b) (filled circle) and (c) (×) is plotted against W. The solid line follows the Crooks relation for the exact β and ΔF. A best fit of the function $\exp(AW - B)$ for the noisy spectrum in (c) gives $A = 0.72/\omega_0$ and $B/A = 0.20\omega_0$, compared to the exact values $\beta = 0.69/\omega_0$ and $\Delta F = 0.22\omega_0$, respectively.

The analysis is completed by extracting the amplitudes of all identifiable peaks in $P_F(W)$ and $P_B(W)$ and computing the ratio $P_F(W)/P_B(-W)$ for these energies. The Crooks relation Eq. (2) predicts that these lie on a exponential curve, which is plotted as a straight line on a logarithmic scale in Fig. 2(d) for the exact β and ΔF of the quench. The extracted ratios for the three examples given in Figs. 2(a) and 2(c) are also plotted and found to cluster tightly on this line. For each case, a fitting to $\exp(AW - B)$ is made with the parameter A providing an estimate of β, thereby establishing that the interferometric protocol also acts as a thermometer. Using A, the fit parameter B/A subsequently allows an estimate of ΔF to be extracted. For the data in Figs. 2(a) and 2(b) the fittings essentially yield the exact result $\Delta F = \epsilon_\sigma(t_R) - (1/2)g_\sigma(t_R)^2/\omega_0$, demonstrating the independence of the Crooks relation from the details of the quench protocol. The noisy spectra in Fig. 2(c) also provides a good estimate of both β and ΔF from its zeroth- and first-order peaks (see caption).

Discussions and conclusions.—We have outlined an experimental scheme employing Ramsey interferometry of a single probe qubit to extract the full statistics of work done on a closed quantum system. We have demonstrated the feasibility of our scheme using a conventional ion-trap arrangement and standard tools for laser manipulation under realistic conditions. As such, our proposal should pave the way for the first experimental verification of nonequilibrium fluctuation relations in the quantum regime. Furthermore, our scheme is generally applicable to a range of current quantum technologies and may be used to probe many-body systems, in which the statistics of work can shed light on universal critical properties of the system [25–27].

The authors thank M. Paternostro for informative discussions on the topic of this work. We also thank U. Poschinger, A. Alberti, and S. Deffner for helpful comments on an earlier version of the manuscript. R. D. is funded by the EPSRC; J. G. acknowledges funding from IRCSET through a Marie Curie International Mobility fellowship; S. R. C., L. H., R. F., and V. V. thank the National Research Foundation and the Ministry of Education of Singapore for support; V. V. received support of a fellowship from Wolfson College Oxford and is also supported by the John Templeton Foundation and the Leverhulme Trust (UK).

*rd309@ic.ac.uk

[1] C. Jarzynski, Annu. Rev. Condens. Matter Phys. **2**, 329 (2011).
[2] C. Jarzynski, Phys. Rev. Lett. **78**, 2690 (1997).
[3] C. Jarzynski, J. Stat. Mech. (2004) P09005.
[4] G. E. Crooks, Phys. Rev. E **60**, 2721 (1999).
[5] D. Collin, F. Ritort, C. Jarzynski, S. B. Smith, I. Tinoco, and C. Bustamante, Nature (London) **437**, 231 (2005); A. N. Gupta, A. Vincent, K. Neupane, H. Yu, F. Wang, and M. T. Woodside, Nat. Phys. **7**, 631 (2011).
[6] M. Campisi, P. Hänggi, and P. Talkner, Rev. Mod. Phys. **83**, 771 (2011).
[7] H. Tasaki, arXiv:cond-mat/0009244; J. Kurchan, arXiv:cond-mat/0007360v2; S. Mukamel, Phys. Rev. Lett. **90**, 170604 (2003).
[8] G. Huber, F. Schmidt-Kaler, S. Deffner, and E. Lutz, Phys. Rev. Lett. **101**, 070403 (2008).
[9] A. Recati, P. O. Fedichev, W. Zwerger, J. von Delft, and P. Zoller, Phys. Rev. Lett. **94**, 040404 (2005).
[10] M. Bruderer and D. Jaksch, New J. Phys. **8**, 87 (2006).
[11] J. Goold, T. Fogarty, N. LoGullo, M. Paternostro, and T. Busch, Phys. Rev. A **84**, 063632 (2011).
[12] A. Sindona, J. Goold, N. Lo Gullo, S. Lorenzo, and F. Plastina, arXiv:1211.1398.
[13] D. Rossini, T. Calarco, V. Giovannetti, S. Montangero, and R. Fazio, Phys. Rev. A **75**, 032333 (2007).
[14] J. D. Baltrusch, C. Cormick, G. De Chiara, T. Calarco, and G. Morigi, Phys. Rev. A **84**, 063821 (2011).
[15] L. Mazzola, G. De Chiara, and M. Paternostro, Phys. Rev. Lett. **110**, 230602 (2013).
[16] M. Campisi, P. Talkner, and P. Hänggi, Phil. Trans. R. Soc. A **369**, 291 (2010).
[17] P. Talkner, E. Lutz, and P. Hänggi, Phys. Rev. E **75**, 050102R (2007).
[18] The condition $t_R > t_Q$ allows $\chi_F(u)$ to be calculated only on the positive real axis, i.e., $u \geq 0$. However, since $P_F(W)$ is a real function, we have $\chi_F(-u) = \chi_F^*(u)$ and only the real and imaginary parts of χ_F on the half-axis are required to fully construct $P_F(W)$.
[19] D. Liebfried, R. Blatt, and C. Monroe, Rev. Mod. Phys. **75**, 281 (2003).
[20] S. A. Gardiner, J. I. Cirac, and P. Zoller, Phys. Rev. Lett. **79**, 4790 (1997).
[21] M. J. McDonnell, J. Home, D. Lucas, G. Imreh, B. Keitch, D. Szwer, N. Thomas, S. Webster, D. Stacey, and A. Steane, Phys. Rev. Lett. **98**, 063603 (2007).
[22] The Stark shifts for the $|\uparrow\rangle$ and $|\downarrow\rangle$ states are absorbed into the qubit splitting Δ, which we assume is accounted for prior to Fourier transforming.
[23] U. Poschinger, A. Walther, K. Singer, and F. Schmidt-Kaler, Phys. Rev. Lett. **105**, 263602 (2010).
[24] Q. A. Turchette, C. J. Myatt, B. E. King, C. A. Sackett, D. Kielpinski, W. M. Itano, C. Monroe, and D. J. Wineland, Phys. Rev. A **62**, 053807 (2000).
[25] A. Silva, Phys. Rev. Lett. **101**, 120603 (2008).
[26] R. Dorner, J. Goold, C. Cormick, M. Paternostro, and V. Vedral, Phys. Rev. Lett. **109**, 160601 (2012).
[27] P. Smacchia and A. Silva, Phys. Rev. Lett. **109**, 037202 (2012); A. Gambassi and A. Silva, Phys. Rev. Lett. **109**, 250602 (2012).
[28] V. Giovannetti, S. Lloyd, and L. Maccone, Nat. Photonics **5**, 222 (2011).